Subsonic choked flow in the microchannel

Xie Chong[a)]
Key Laboratory of High Temperature Gas Dynamics, Institute of Mechanics of the Chinese Academy of Sciences, 15 West Road, North 4th Circle, Beijing 100080, China

(Received 2 March 2006; accepted 27 October 2006; published online 27 December 2006)

Choked gas flows in the microchannel were studied. With use of the direct simulation Monte Carlo (DSMC) method, a serial of microchannels (length $L=10$, 100, and 200 μm) was simulated and gained a flow-field evolutional trend with pressure ratio. Also, the effects of the boundary condition setting on the mass flux and static pressure distribution were analyzed during the nonequilibrium flows. It is shown that for the microchannel, the sonic point (Ma=1) only appears at the center point of the outlet section when it is choked. Finally, this paper compares the mass flux between the isothermal limiting Navier-Stokes (NS) and DSMC results, and it is concluded that the limiting NS result can be used to estimate the mass flux when the length of the channel is very long (the ratio of length to height is larger than 1000). © *2006 American Institute of Physics.*
[DOI: 10.1063/1.2408510]

I. INTRODUCTION

Since the 1980s, great progress has been made in microelectromechanical systems (MEMS) technology. Researchers have been drawn to this technology not only for the potential of the MEMS process, but also because of its many characteristic physical phenomena. The microchannel with a rectangular section is one of the main geometrical units in MEMS, and its gas flows have attracted the attention of many researchers.[1–11] Their work has been focused mainly on the isothermal (e.g., flow Mach number $\mathrm{Ma} \ll 1$) gas flows, the heat transfer between gas flow and channel walls when there was a temperature difference, and the nonisothermal effect that comes from high-speed flow ($\mathrm{Ma} > 0.3$). Generally, the following two points have been widely accepted. (i) Because the ratio of surface area to volume increases rapidly with the decrease of device dimension, the interaction between the fluid and wall should be important. For microchannel gas flows, it embodies the strong friction that wall hold back gas movement. So even if the average flow speed is very small (less than 1 m/s), there should be an obvious compression of fluid. (ii) When the characteristic dimension H (the height of the channel in the microchannel) of a microdevice can compare with the mean free path λ of a gas molecule, then the rarefied gas effect should appear gradually, such as, e.g., the phenomena of velocity slip and temperature jump at walls. For those phenomena, the assumption of a continual medium should break down gradually.[13] In the rarefied gas dynamics field, one important nondimensional Knudsen number is defined by

$$\mathrm{Kn} = \lambda/H. \tag{1}$$

The above two factors created many new phenomena of microdimensional gas flows.

The flows driven by pressure that are added to the inlet and outlet of the microchannel have some interesting characteristics that differ from the macroscopic channel. As is well known, the flow velocity should increase with the increase of the pressure ratio. For the macroscopic channel, the pressure can drive the velocity to the local sonic speed (Ma=1) at the outlet section (except the near wall) of the channel. Then if one again increases the pressure, the back conditions will not change the inner flow character of the channel, and the mass flux will achieve its maximum. This kind of phenomenon is known as choked flow, and all of the inner channel flow is subsonic. Some researchers have analyzed this flow in the microchannel.[9–11] In this paper, the short (channel length $L=10$ μm) and moderately long ($L=100$ μm and $L=200$ μm) two-dimensional microchannel gas flows are studied. By always setting the total pressure to about 1.01×10^5 Pa in the region of the inlet and reducing it from 1 atm to $100-1000$ Pa at the region of the outlet, we observed the evolutional process of choking. This kind of flow can usually be found in the emission of the micromass of reactive gas, which is a process of functional material and of some gas in the outer space. It may also appear in mass transmission and heat transformation of MEMS. At the same time, this work observes the effect of the boundary condition setting on the results, and illustrates that the boundary setting is pivotal when the flow occurs in a choked state with nonequilibrium.

II. SIMULATIVE CONDITIONS AND METHODS

Because of the large ratio of the channel's width W to height H ($W/H > 50$) (Refs. 1–5) in practical usage, the three-dimensional rectangular channel can be simplified as a two-dimensional model (in length and height). Figure 1 shows a two-dimensional sketch of the simulative channel. Line $AA'B'B$ is the outline of the microchannel, AB is the inlet, and $A'B'$ is the outlet. $EFCD$ and $F'E'D'C'$ are the neighboring regions of the inlet and the outlet, respectively, and the lines AA', AF, $A'F'$, BB', BC, and $B'C'$ are walls. OO' is a symmetrical line of the whole channel. For isother-

a)Electronic mail: ChongXie@263.net

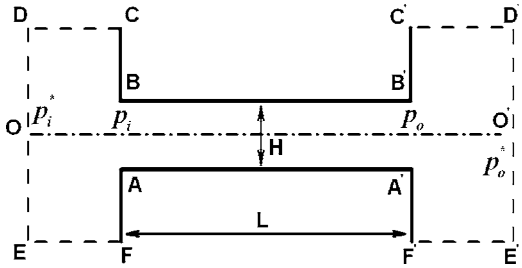

FIG. 1. Sketch map of computational regions.

mal flow in the setting of the flow boundary, see Refs. 14–16. For choked flow, the variety of temperature should be evident. When the simulated region is limited within $AA'B'B$, if one applies the flow boundary condition by extrapolation, it may distort the physical reality and lessen the precision of the results. To overcome this, in this paper we add two buffer regions $EFCD$ and $F'E'D'C'$, and set the flow boundary condition at $CDOEF$ and $C'D'O'E'F'$. With the proper geometrical choice of the buffer region, the simulative gains (for example, static pressure and temperature) will match the setting ones consistently. Initially, the total pressure p_i^* and p_o^* is set at two ports, after which gas starts to flow from left to right. To observe the difference in the results with and without the buffer regions, the latter must also be simulated to ensure the same total pressure at inlet AB. When the simulated molecules enter into the calculational region, the assumption of equilibrium (e.g., Maxwell's distribution) is used. The free flow gas and walls have the same temperature, 295 K, and the fluid is argon or air. Finally, in thinking about the symmetry of geometry, only the underside region of line OO' is simulated.

Since the 1970s, the direct simulation Monte Carlo (DSMC) method[12] has been developed extensively. It is now widely used in many flow problems with the rarefied gas effect, so it can be used reliably to deal with the near sonic speed microchannel choked flows. The main DSMC methods in this paper are according to Refs. 14–16. Because of the lower change of temperature in the whole flow field, the collision model VHS (Ref. 12) was used. The choice of collision pair adopts the NTC (Ref. 12) method.

III. RESULTS AND ANALYSIS

To explain the difference between factual choked flow and the isothermal assumption, we use Arkilic *et al.*'s analytical resolution,[3] which considers the NS equation adding a one-order velocity slip boundary condition. By reducing the two-dimensional isothermal steady NS equations and using the boundary condition at the wall,

$$u|_w = \left(\frac{2-\sigma}{\sigma}\right)\lambda \left.\frac{\partial u}{\partial y}\right|_w, \tag{2}$$

the velocity distribution in the whole microchannel and the pressure distribution along the flow direction can be gained. Then with the product of velocity and density along the flow direction, we get the mass flux expression,

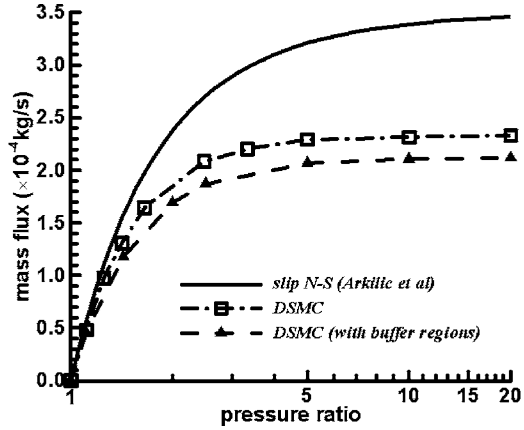

FIG. 2. Comparison of mass flux of choked gas flows in a short channel.

$$Q = \frac{H^3 p_o^2}{24\mu LRT}\left(\Pi^2 - 1 + 12\frac{2-\sigma}{\sigma}\mathrm{Kn}_o[\Pi - 1]\right). \tag{3}$$

$\Pi = p_i/p_o$ is the static pressure ratio of inlet to outlet. The subscript o represents the outlet of the channel, and σ is the TMAC (tangential momentum accommodation coefficient), which shows (from the view of statistics) the degree of accommodation when incident molecules collide with the wall and then reflect from it. It may be valued from 0 (mirror reflection) to 1 (diffuse reflection). Considering the broad usage of diffuse reflection in the field of engineering and the good results that are achieved when applying it to the microchannel's low-speed flow, the diffusion reflection $\sigma = 1.0$ is used in the DSMC and NS results. μ, R, and T are the viscous coefficient, gas constant, and temperature, respectively. Interestingly, the mass flux in formula (3) will not increase much and it has a limiting mass flux expression when p_i is fixed and p_o goes to zero. Conveniently, formula (3) can be changed to

$$Q = \frac{H^3 p_i^2}{24\mu LRT}\left\{\left(1 - \frac{1}{\Pi^2}\right) + 12\frac{2-\sigma}{\sigma}\frac{\mathrm{Kn}_o}{\Pi}\left[1 - \frac{1}{\Pi}\right]\right\}, \tag{4}$$

when $\Pi \to +\infty$ and considering the mean free path expression of the hard-sphere molecular model,[12,13]

$$\lambda_o = \frac{16}{5}\sqrt{\frac{kT}{2\pi m}}\frac{\mu}{p_o}. \tag{5}$$

The limiting expression of mass flux is

$$Q|_{\Pi\to+\infty} = \frac{H^3 p_i^2}{24\mu LRT}\left(1 + 12\frac{2-\sigma}{\sigma}\frac{\mu}{p_i H}\frac{16}{5}\sqrt{\frac{kT}{2\pi m}}\right), \tag{6}$$

where m is the molecular mass and k is Boltzmann's constant. Because the mass flux increases monotonously with the increase of Π, formula (6) is the isothermal maximum of mass flux.

Figure 2 shows the evolution of mass flux versus ratio of pressure. At the inlet section AB, all the methods (NS, DSMC that only simulated the channel's region $AA'B'B$, and DSMC that included the two buffer regions) have the same average total pressure. In this serial of cases, the channels $L = 10$ μm, $H = 2$ μm, and the gas is argon. The abscissa of

Fig. 2 is the ratio of the inlet's total pressure to the outlet's static pressure. The figure displays clearly the discrepancy of the mass flux of the three methods when flow moves gradually into the choked state. Compared with the isothermal NS results, the choked rarefied gas flows included two main characters as follows: (i) With a decrease of the outlet's static pressure, under some conditions the Knudsen number, which will increase near the outlet, can reach the transition regime of near free molecular flow. (ii) According to the accelerated flow, the static temperature of the gas will vary, e.g., the transform between kinetic and inner energy. At the same time, the viscous dissipation will be strengthened. From the existing conclusion about low-speed rarefied gas channel flow,[1–5,8] the rarefied effect can admit more mass flux than the NS result. This is contrary to the relation in Fig. 2, so it implies that viscous dissipation plays a dominant role in this choked flow. Also, we take notice of the smaller difference (relative error about 8%) between the two DSMC results in Fig. 2. The possible reasons for this will be proposed in the next paragraph.

Figure 3 shows a serial of contours of the physical field when choked flow occurred. All results are derived from DSMC with buffer regions. Line $y=1$ is symmetrical to line OO'. Figure 3(a) is Mach contour, and similar to the macroscopic choked channel, the position of Ma=1 appears at the outlet section. But because of the strong wall's friction that held back flow in spite of the strong velocity slip at the wall, the ultimate sonic speed only appears at the center point of the outlet. After the gas passes through the outlet, it will undergo a process of expansion (like a vacuum plume). This phenomenon can be explained by Fig. 3(f). In this simulated case, the static pressure of $C'D'O'E'F'$ was set to 5000 Pa, however at the outlet the average static pressure is about 21000 Pa. In other words, the total difference in pressure cannot be attributed entirely to the whole channel after the gradual appearance of choked flow. This phenomenon is important when dealing with the microdevice experimental data. Limited by the geometry of microdevices, it is inconvenient to place many sensors in them. In most cases, the data measured near the outlet are regarded in the same way as the data of the outlet section. This can sometimes lead to errors and even wrong conclusions when choked flow appears. Figure 3(b) shows the distribution of the average translational kinetic temperature. According to the maximal Mach number, the temperature falls to the minimal value. Figure 3(e) shows the mass density distribution. Due to nonisothermal flow, at the same x position the density varies with y. From the above analyses, we can suggest some reasons to explain why the two DSMC method's results (with and without buffer regions) differ (see Fig. 2). First of all, the outlet's static pressure for the single channel's DSMC (without buffer regions) can be set to any value, but practically it only reaches some limiting value. The set pressure (less than that limiting value) would decrease artificially the molecule numbers that should enter the simulative domain from the outlet. Second, at two ports of the channel, especially at the outlet's neighborhood, there exist larger grades of physical variables (velocity, temperature, and pressure). It forms a nonequilibrium relaxation phenomenon. the setting of the

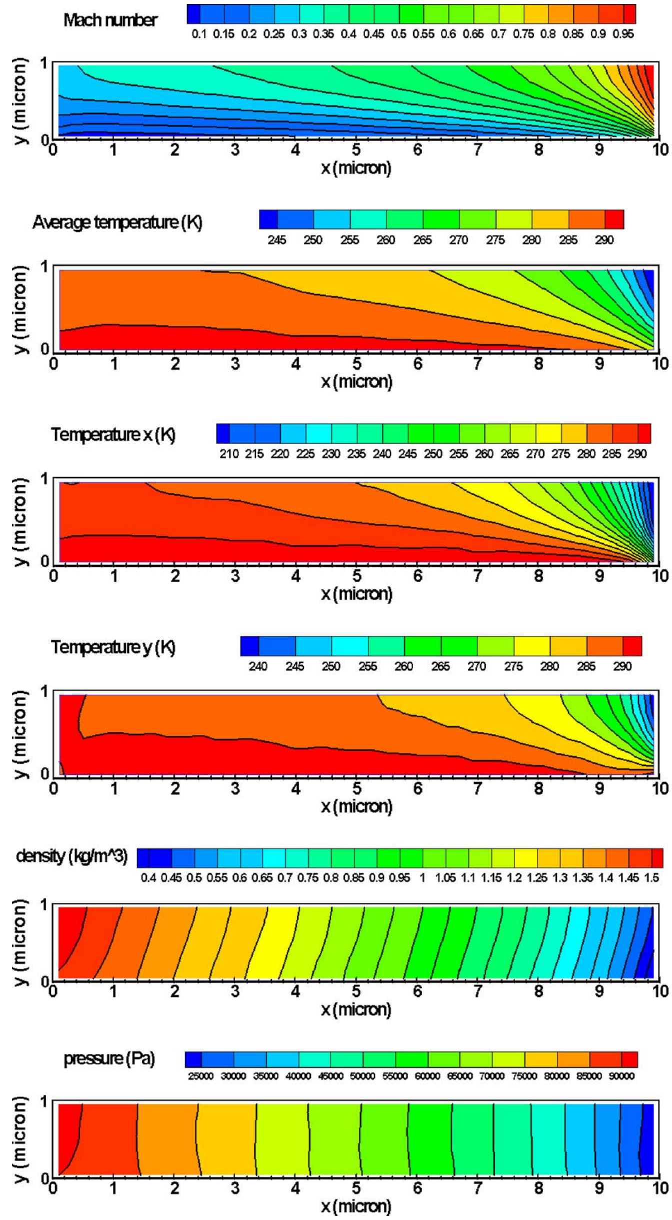

FIG. 3. Flow-field variable contours gained from a simulated short channel with buffer regions. (a) Mach number contour, (b) average translational kinetic temperature contour, (c) X-directional translational kinetic temperature contour, (d) Y-directional translational kinetic temperature contour, (e) mass density contour, and (f) static pressure contour.

equilibrium Maxwell condition cannot describe boundary flows accurately. Figures 3(c) and 3(d) show translational kinetic temperatures at the x and y directions, respectively. They provide proof of the nonequilibrium of gas flows.

To explain further the effect of the boundary condition on the results, we also compare the static pressure distribution of small-channel choked flows.[10,11] In Ref. 11, the tested channel has length $L=150$ mm, width $W=32$ mm, and height $H=0.7$ mm. The gas is air. By turning the vacuum valve, the total pressure of the channel inlet can be set to any value, and the outlet is connected to a very low constant pressure vacuum tank. This small channel ($H=0.7$ mm) can have a similar Knudsen number to the microchannel $[H \approx O(1\ \mu\text{m})]$ region. Reference 10 compared the simulative

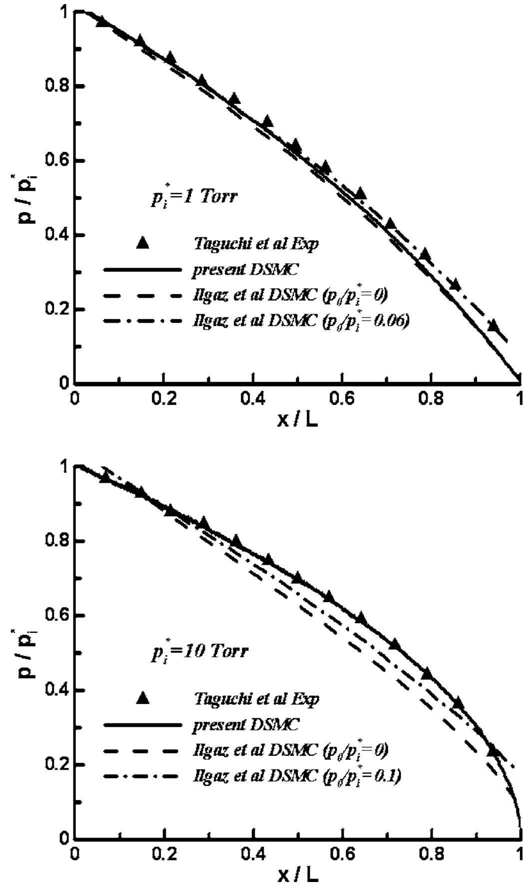

FIG. 4. Comparison of Ilgaz *et al.*'s DSMC, present simulation, and experimental data for static pressure distribution. (a) Inlet total pressure is 1 Torr. (b) Inlet total pressure is 10 Torr.

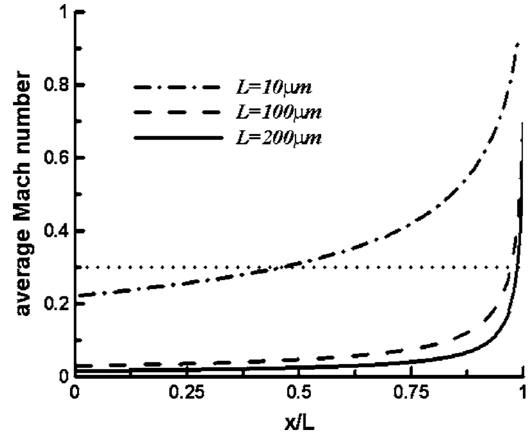

FIG. 5. Average Mach number along non-dimensional flow direction for short and moderate long micro-channels.

pressure distribution with experimental data. In Ref. 10, the authors simulated only a single channel (i.e., without buffer regions). In order to obtain the desired results, the finite backpressure p_o was set artificially at the outlet section. In Fig. 4, the results of two experimental cases (inlet total pressure 1 and 10 Torr, respectively) are shown. In the figure, the present DSMC used buffer regions, and the outlet region $C'D'O'E'F'$ (in Fig. 1) was set to absolute vacuum (0 Pa). The good agreement shows that the present DSMC can gain flow character naturally.

Generally, the experimental and engineering microchannels have a very large length. If the main flow region in the channel is isothermal and belongs to the regime in which the continuum model is valid, then the isothermal NS model can be used as an engineering reference. To validate the above analysis, Fig. 5 shows the averaged Mach number (geometric mean at every section) along the length; the three simulated choked cases ($L=10$, 100, and 200 μm) were compared. From this figure, we can see that for the 200 μm length case the high-speed ($\mathrm{Ma} \geqslant 0.3$) domain is only limited to the very small region near the outlet. Thus the temperature change caused by the violent viscous dissipation and acceleration only takes place in that area. The main region (from the inlet to near the outlet) should be low-speed isothermal flow. The main decrease of pressure also takes place in that low-speed flow region. If someone wants to know the choked mass flow, the isothermal NS limiting result [formula (6)] can be used as a reference. As proof, in the above three cases the mass flux was also compared. Using formula (6) as Q_{NS}, the relative error $[(Q_{\mathrm{NS}}-Q_{\mathrm{DSMC}})/Q_{\mathrm{NS}}]$ is 45.7% for $L=10$ μm, it falls to 11.2% if $L=100$ μm, and it falls to 5.7% if $L=200$ μm. By extrapolation we can predict that the relative error can be controlled under 2% if L is larger than 1000 μm. With use of experimental data, the above conclusion can be accepted as evident. For Refs. 17 and 18, the test microchannel $L=39.9$ mm, $H=7$ μm, and $W=1000$ μm. The degree of roughness of the surface is 2%. As a result of the very large ratio of width to height, the two-dimensional model should be proper. The inlet pressures were set to 130, 250, and 320 kPa, respectively, and the outlet connects to the vacuum system. The vacuum system can offer a backpressure environment that falls gradually to 10 kPa. Even if the outlet's pressure is equal to 10 kPa, the Knudsen number in the whole channel would be less than 0.1, so the results with the assumption of a continual medium can be used. The experiment measured the mass flux and pressure distribution along the channel. Figure 6 compares the measured choked mass flux with the results of the NS method [also using formula (6)]. All relative errors are less than 2%.

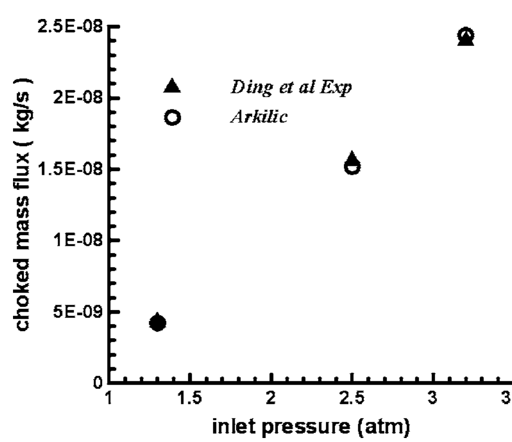

FIG. 6. Comparison of experimental choked mass flux with Arkilic *et al.*'s limiting results.

IV. CONCLUSIONS

The detailed field distributions of microchannel choked gas flows were studied. As a result of the pressure difference, for the constant section microchannel, the maximum Ma=1 only appears at the center point of the outlet when the choked flow appears. The increase of velocity in the non-equilibrium phenomenon at the port region cannot be ignored. The region that has an obvious nonisothermal effect is near the outlet of the channel, and for a very long microchannel, the isothermal NS results can be used as an approximate reference (relative error less than 2%).

[1] Y. Zohar, S. Y. K. Lee, W. Y. Lee, L. Jiang, and P. Tong, "Subsonic gas flow in a straight and uniform microchannel," J. Fluid Mech. **472**, 257 (2002).
[2] J. Maurer, P. Tabeling, P. Joseph, and H. Willaime, "Second-order slip laws in microchannels for helium and nitrogen," Phys. Fluids **15**, 2613 (2003).
[3] E. B. Arkilic, K. S. Breuer, and M. A. Schmidt, "Mass flow and tangential momentum accommodation in silicon micromachined channels," J. Fluid Mech. **437**, 29 (2001).
[4] K. C. Pong, C. M. Ho, J. Q. Liu, and Y. C. Tai, "Non-linear pressure distribution in uniform micro-channels," Proceedings ASME-FED **197**, 51 (1994).
[5] J. C. Shih, C. M. Ho, J. Liu, and Y. C. Tai, "Monatomic and polyatomic gas flow through uniform microchannels," Proceedings ASME-DSC **59**, 197 (1996).
[6] C. S. Chen, S. M. Lee, and J. D. Sheu, "Numerical analysis of gas flow in microchannels," Numer. Heat Transfer, Part A **33**, 479 (1998).
[7] C. K. Oh, E. S. Oran, and R. S. Sinkovits, "Computations of high-speed, high Knudsen number microchannel flows," J. Thermophys. Heat Transfer **11**, 497 (1997).
[8] C. Mavriplis, J. C. Ahn, and R. Goulard, "Heat transfer and flowfields in short microchannels using direct simulation Monte Carlo," J. Thermophys. Heat Transfer **11**, 489 (1997).
[9] W. Shi, M. Miyamoto, Y. Katoh, and J. Kurima, "Choked flow of low density gas in a narrow parallel-plate channel with adiabatic walls," Int. J. Heat Mass Transfer **44**, 2555 (2001).
[10] M. Ilgaz and M. C. Celenligil, "DSMC simulations of low-density choked flows in parallel-plate channels," in *23rd International Symposium on Rarefied Gas Dynamics*, edited by A. D. Ketsdever and E. P. Muntz, AIP Conf. Proc. No. 663 (AIP, New York, 2003).
[11] T. Taguchi, K. Yanagi, M. Miyamoto, and T. Nagata, "Precise discharge characteristic of rarefied critical flows through a parallel plate channel," in *19th International Symposium on Rarefied Gas Dynamics*, edited by J. Harvey and G. Lord (Oxford University Press, Oxford, 1995).
[12] G. A. Bird, *Molecular Gas Dynamics and the Direct Simulation of Gas Flow* (Clarendon, Oxford, 1994).
[13] Q. Shen, *Rarefied Gas Dynamics* (Springer, New York, 2005).
[14] C. Xie, J. Fan, and Q. Shen, "Rarefied gas flows in micro-channels," Chin. J. Comput. Phys. **19**, 377 (2002) (in Chinese).
[15] C. Xie, J. Fan, and C. Shen, "Statistical simulation of rarefied gas flows in micro-channels," in *23rd International Symposium on Rarefied Gas Dynamics*, edited by A. D. Ketsdever and E. P. Muntz, AIP Conf. Proc. No. 663 (AIP, New York, 2003).
[16] C. Shen, J. Fan, and C. Xie, "Statistical simulation of rarefied gas flows in micro-channels," J. Comput. Phys. **189**, 512 (2003).
[17] Y. T. Ding, F. He, Z. H. Yao, M. Y. Shen, and X. F. Wang, "Sub-choking phenomenon of low-speed gas flow in a long-constant-area microchannel," Acta Phys. Sin. **53**, 2429 (2004) (in Chinese).
[18] X. M. Sun, F. He, and Y. T. Ding, "Application of BGK scheme on microchannel gas flow," Chin. Phys. Lett. **20**, 2199 (2003).